1-1-1979

Optimization of Detector-Preamplifier for Cryogenic Spectrometry

D. Gary Frodsham

Doran J. Baker

'91, 130 - 134 (1979)
Frodsham, D. Gary, and Doran J. Baker. 1979. "Optimization of Detector-Preamplifier for Cryogenic Spectrometry." *Proceedings of SPIE* 0191: 130–34. doi:10.1117/12.957824.

Optimization of detector-preamplifier for cryogenic spectrometry

D. Gary Frodsham and Doran J. Baker
Electro-Dynamics Laboratories
Electrical Engineering Department
Utah State University
Logan, Utah 84322

Abstract

The design optimization of the detector-preamplifier subsystem is critical to the achievement of sensitive infrared spectrometers. The application illustrated is for cryogenically-cooled detectors, but the optimal approach based upon an operational preamplifier is general for detector operation under background limited conditions.

Introduction

For many years the stability characteristics of the negative-feedback operational amplifier have been exploited in the engineering of optical measurement systems [Baker *et al.*, 1964]. In designing infrared spectrometers for in-the-field measurements, optimal tradeoffs of minimum detectable signal, speed of response, and dynamic range are critical. In many cases there is no opportunity for repeating the experiment.

In the design optimization the detector and its signal-conditioning preamplifier are treated as a single subsystem. The approach is to solve for a range of load resistor values which produce a minimum noise equivalent power for any given dynamic range and bandwidth requirement. Both compensated and uncompensated frequency response subsystems are treated.

Detector-Preamplifier Configuration

The configuration of a widely-used detector-preamplifier is given in Figure 1.

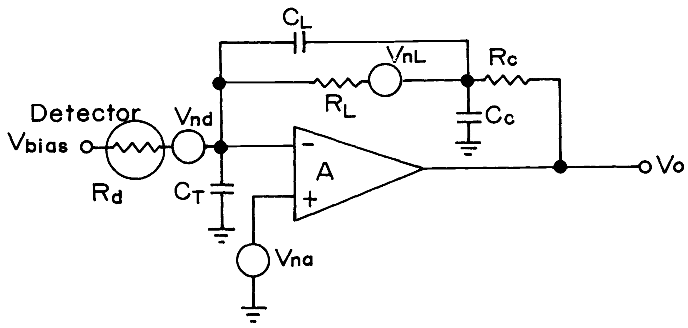

Figure 1. Configuration model for detector/preamplifier subsystem used in infrared spectrometer.

The negative feedback elements of the operational preamplifier of open loop gain A are shown as R_L and C_L. The distributed stray capacitance along the body of R_L is difficult to compensate in order to achieve the desired bandwidth characteristics. Therefore, a shunt external capacitance C_L is added externally to dominate this stray capacitance. The components R_c and C_c are then added as shown to compensate for the roll-off of the feedback elements R_L, C_L.

The capacitance C_T is given by $C_T = C_d + C_{in}$. The value of C_d is the capacitance associated with the detector and C_{in} is that inherent in the preamplifier including stray capacitance.

The thermal noises of the detector-preamplifier subsystem are modeled as series voltage sources as included in Figure 1. The noise voltage associated with the detector resistance R_d is designated V_{nd}, that associated with the feedback resistor R_L is designated V_{nL}, and V_{na} is the equivalent input noise produced by the operational preamplifier A.

It can be shown that the foregoing thermal noise sources produce noise at the output of the preamplifier of the form summarized in Table 1. In deriving these relationships it was assumed that the magnitude of the input impedance of the operational preamplifier is much greater than either the detector resistance R_d or the feedback resistance R_L. The open loop gain A of the preamplifier is a function of the frequency ω expressed in radians/second.

Table 1. Preamplifier noise outputs

Source	Uncompensated Case ($R_cC_c = 0$)	Frequency - Compensated Case ($R_LC_L = R_cC_c$)
Detector	$V_{ndo} = -V_{nd}\left(\frac{R_L}{R_d}\right)\left[\frac{1}{j\omega R_L\left(C_L + \frac{C_T}{A}\right) + \left(\frac{R_L + R_d}{AR_d}\right) + 1}\right]$	$V_{ndo} = -V_{nd}\left(\frac{R_L}{R_d}\right)\left[\frac{1}{j\omega R_L\left(\frac{C_L + C_T}{A}\right) + \left(\frac{R_L + R_d}{AR_d}\right) + 1}\right]$
Feedback Resistor	$V_{nLo} = V_{nL}\left[\frac{1}{j\omega R_L\left(C_L + \frac{C_T}{A}\right) + \left(\frac{R_L + R_d}{AR_d}\right) + 1}\right]$	$V_{nLo} = V_{nL}\left[\frac{1}{j\omega R_L\left(\frac{C_L + C_T}{A}\right) + \left(\frac{R_L + R_d}{AR_d}\right) + 1}\right]$
Pre-amplifier	$V_{nao} = -V_{na}\left[\frac{j\omega R_L(C_L + C_T) + \left(\frac{R_L + R_d}{R_d}\right)}{j\omega R_L\left(C_L + \frac{C_T}{A}\right) + \left(\frac{R_L + R_d}{AR_d}\right) + 1}\right]$	$V_{noa} = -V_{na}\left[\frac{j\omega R_L(C_L + C_T) + \left(\frac{R_L + R_d}{R_d}\right)}{j\omega R_L\left(\frac{C_L + C_T}{A}\right) + \left(\frac{R_L + R_d}{AR_d}\right) + 1}\right]$

For most applications, the frequencies of interest are inherently below the breakpoint for the roll-off of the detector-preamplifier combination. As a consequence, the terms

$$\left[j\omega R_L\left(C_L + \frac{C_T}{A}\right) + \left(\frac{R_L + R_d}{AR_d}\right) + 1\right] \approx 1 \quad \text{(uncompensated)} \tag{1}$$

and

$$\left[j\omega R_L\left(\frac{C_L + C_T}{A}\right) + \left(\frac{R_L + R_d}{AR_d}\right) + 1\right] \approx 1 \quad \text{(compensated)} . \tag{2}$$

Therefore we can simplify the equations of Table 1 and rewrite them respectively as

$$V_{ndo} = -V_{nd}R_L/R_d \quad , \tag{3}$$

$$V_{nLo} = V_{nL} \quad , \tag{4}$$

$$V_{nao} = -V_{na}\left[j\omega R_L(C_L + C_T) + (R_L + R_d)/R_d\right] . \tag{5}$$

The Johnson thermal model is $V_{nj} = (4kTR)^{\frac{1}{2}}$, where $k = 1.38 \times 10^{-23}$ JK^{-1}, and T and R are the absolute temperature and resistance, respectively. Using this model for the thermal noise associated with the detector and feedback resistances, respectively, gives

$$V_{ndo} = -(R_L/R_d)(4kTR_d)^{\frac{1}{2}} \tag{6}$$

$$V_{nLo} = (4kTR_L)^{\frac{1}{2}} \quad . \tag{7}$$

The effects of the bandwidth on the noise can be taken into account using

$$V_n(\text{RMS}) = \left[\int_{f_1}^{f_2} F(R_L)^2 df\right]^{1/2} \quad (8)$$

From an integration of this rms voltage formula using the foregoing relations it can be shown that

$$V_{ndo} = \left[\left(R_L/R_d\right)\ 4kTR_d(f_2 - f_1)\right]^{1/2} \quad (9)$$

$$V_{nLo} = \left[4kTR_L(f_2 - f_1)\right]^{1/2} \quad (10)$$

$$V_{nao} = V_{na}\left[\left[(2\pi R_L) \times (C_L + C_T)\right]^2 \left[(f_2^3 - f_1^3)/3\right] + \left[(R_d + R_L)/R_d\right]^2 (f_2 - f_1)\right]^{1/2}. \quad (11)$$

The total noise V_{nt}(RMS) contributed by all three noise sources by the additive relationship

$$V_{nt} = \left[(V_{ndo})^2 + (V_{nLo})^2 + (V_{nao})^2\right]^{1/2} \ . \quad (12)$$

Substituting equation (9), (10), and (11) into (12)

$$V_{nt} = R_L\left[\left[4kT(1/R_L + 1/R_d) + V_{na}^2(1/R_L + 1/R_d)^2\right](f_2 - f_1) + \left[V_{na}2\pi(C_L + C_T)\right]^2 \frac{(f_2^3 - f_1^3)}{3}\right]^{1/2} \quad (13)$$

To derive the noise equivalent power NEP of the detector-preamplifier subsystem, we use the defining relationship (in watts)

$$\text{NEP} = V_{nt}/(R_\lambda R_L) \quad , \quad (14)$$

where R_λ is the detector responsivity (amps/watt) as a function of optical wavelength λ. Substitution of equation (13) into (14) gives

$$\text{NEP} = (1/R_\lambda)\left[\left[4kT(1/R_L + 1/R_d) + V_{na}^2(1/R_L + 1/R_d)^2\right](f_2 - f_1) + \left[V_{na}2\pi(C_L + C_T)\right]^2 \frac{(f_2^3 - f_1^3)}{3}\right]^{1/2}. \quad (15)$$

Equation (15) expresses the sought for value of NEP for the detector-preamplifier configuration combination as described by Figure 1. This relationship is valid for the case where thermal rather than photon noise predominates in the system. In the derivation of Equation (15), the amplifier noise voltage V_{na} was approximated as constant. For the JFET type devices being used in state-of-the-art preamplifiers, the assumption was found to be valid at frequencies down to about 100 Hz. At 10 Hz a value for V_{na} of 2×10^{-8} V/Hz$^{1/2}$ was measured which, of cource, increases with decrease of frequency as 1/f. However, it can be shown from Equation (13) that the output noise density at the lower frequencies, where the 1/f characteristic of V_{na} is present, is dominated by the thermal noise associated with the R_L and (or) R_d. Thus, the assumption that V_{na} is constant is valid for this derivation of Equation (15).

Optimization

The analysis of the detector-preamplifier configuration of Figure 1 will now be applied to the case of an optimal design. The three primary considerations are the frequency requirements f_2 and f_1, noise equivalent power NEP, and dynamic range D_r.

Our optimal approach is to investigate the effect of varying R_L while holding all other parameters constant. We observe from Equation (15) that NEP approaches a minimum (NEP_{min}) as $R_L \to \infty$. However, for practical reasons, it is neither possible nor desirable to make $R_L = \infty$. Furthermore, it is not necessary since we can define a minimum value for R_L such that NEP $\simeq NEP_{min}$.

This minimum value of R_L is ascertained by rewriting Equation (15) in the form

$$\text{NEP} \propto \left(F(R_L) + K\right) \ , \quad (16)$$

where K is used to absorb all the terms independent of R_L and $F(R_L)$ is that function which contains all the terms which are a function of R_L. We then equate $F(R_L)$ to K/4 and solve for the value of $R_L = R(B)$. R(B) then is a "breakpoint" value such that NEP = NEP_{min}. Furthermore, at this value of R_L the NEP is essentially independent of R_L for all values of $R_L \geq R(B)$.

Carrying out the above procedure on Equation (15), we find

$$R(B) = \left[(B^2 - 4AC)^{\frac{1}{2}} - B\right]/2A \quad , \tag{17}$$

where

$$A = \tfrac{1}{4}\left[4kT/R_d + V_{na}^2/R_d{}^2 + (2\pi V_{na})^2/3\left[(f_2^3 - f_1^3)/(f_2 - f_1)\right]\right] , \tag{18}$$

$$B = -\left[4kT + 2V_{na}^2/R_d\right] \quad , \tag{19}$$

$$C = -V_{na}^2 \quad . \tag{20}$$

Having established a lower limit for the magnitude of the feedback resistor R_L, we will now set an upper bound.

The parameter, which establishes the upper bound value of R_L is the desired dynamic range D_r. The dynamic range is defined as the maximum permissible RMS output voltage of the preamplifier divided by the zero signal RMS noise at the output of the preamplifier. This can be written as

$$D_r = (.070)V_o(\text{peak})/2V_{nt} \quad , \tag{21}$$

where V_o is the peak linear output voltage capability of the amplifier A. Typically, V_o is 10 to 12 volts for a ±15 volt system. Thus, a working value for D_r is

$$D_r = 4/V_{nt} \quad . \tag{22}$$

Substituting Equation (22) into Equation (13) and solving for $R_L = R(D)$ gives an upper limit for R_L,

$$R(D) = \left[(B^2 - 4AC)^{\frac{1}{2}} - B\right]/2A \quad , \tag{23}$$

where

$$A = \left[4kT/R_d + V_{na}^2/R_d{}^2 + (2\pi V_{na})^2/3\left[(f_2^3 - f_1^3)/(f_2 - f_1)\right]\right] , \tag{24}$$

$$B = \left[4kT + 2V_{na}^2/R_d\right] \quad , \tag{25}$$

$$C = \left[V_{na} - 16/D_r{}^2(f_2 - f_1)\right] \quad . \tag{26}$$

Finally, it will be recalled that the derivation of Equation (13) was based on the assumption that Equations (1) and (2) are, in practice, valid. There is, of course, a value of R_L for which this is always nearly true. This value of $R_L = R_L(f_2)$ becomes a second upper bound for R_L.

$R_L(f_2)$ is derived by observing that for state-of-the-art amplifiers now in use

$$A \approx \frac{2\pi \times 10^6}{20\pi - j\omega} \quad . \tag{27}$$

Substituting Equation (27) into equation (1) and (2) and solving for $R_L(f_2)$ it can be shown that

$$R_L(f_2) = \frac{10^6}{2\pi f_2^2(C_L + C_T)} \qquad \text{(compensated)} \tag{28}$$

$$R_L(f_2) = \frac{1}{2\pi f_2 C_L} \qquad \text{(uncompensated)} \tag{29}$$

Equations (28) and (29) are valid for the conditions $f_2 \leq 10^6$ and Equation (29) particularly, $f_2 << (C_L/(C_L + C_T)) \times 10^6$.

Conclusions

The use of frequency-compensated, negative-feedback operational preamplifier based upon JFET devices with cryogenically-cooled solid state detectors yields state-of-the-art subsystems for infrared spectrometers [Wyatt, 1975, and Wyatt and Frodsham, 1977]. For detectors operating under background limited conditions, thermal noise dominates the photon shot noise and the optimal negative feedback resistance R_L is bounded by

$$R(D) \text{ and } R(f_2) > R_L > R(B) \quad , \qquad (30)$$

where the values R(B), R(D) and $R(f_2)$ are computed from Equations (17), (23), (28) and (29), respectively.

Upon selection of R_L the noise, NEP, and dynamic range can be computed from Equations (13), (15) and (27), respectively. The pertinent detector parameters for two widely used infrared detectors are given in Table 2. These detectors are doped silicon and indium antimonide.

Table 2. Parameters of doped silicon and alloyed indium-antimonide infrared detectors.

Parameter	Detector: Si(As)	Detector: InSb
Optical Response	2-24 μm	1-5.4 μm
Operational Temperature	4-10° K (LHe)	77-82° K (LN)
Optimum Size	$\leq$ 1 mm^2	$\leq$ 1 mm dia.
Peak Responsivity	$\geq$ 4 amps/watt	$\geq$ 2 amps/watt
Bias Voltage	1-15 volts	---
Detector Capacitance (C_d)	1 pf/side length (mm)	$5 \times 10^{-8} A_d$(cm) farads
Detector Impedance (R_d, low background)	$\geq 10^{15}$ ohms	$\geq 2 \times 10^6/A_d$(cm) ohms

Acknowledgments

The authors acknowledge the assistance of A. T. Stair, Jr., of the Air Force Geophysics Laboratory and of Allan J. Steed and Clair L. Wyatt of the faculty of Utah State University.

References

1. Baker, D.J., C.L. Wyatt and F.R. Brown, Jr., "A Direct-Coupled DC Amplifier Compensated to 20 KC for Use with Photoemissive Devices," IEEE Transactions an Instrumentation and Measurement, Vol. IM-13, Nos. 2 & 3, pp. 115-118; June-September, 1964.
2. Wyatt, C.L., "Infrared Spectrometer: Liquid-helium-cooled Rocketborne Circular-variable Filter," App. Optics, Vol. 14, No. 12, pp. 3086-3091; December, 1975.
3. Wyatt, C.L. and D.G. Frodsham, "Short Wavelength Rocketborne Infrared Spectrometer," Proc. Soc. Photo-Optical Instrumentation Engineers, Vol. 124, pp. 236-243; August 25-26, 1977.